Journal of Peptide Science
J. Peptide Sci. **8**: 347–364 (2002)
Published online in Wiley InterScience (www.interscience.wiley.com). DOI: 10.1002/psc.394

Conformational Solution Studies of (Sar^7)desamino- and (MeAla^7)desamino- Vasopressin Analogues Using NMR Spectroscopy

SYLWIA RODZIEWICZ-MOTOWIDŁO,[a] IGOR ZHUKOV,[b] FRANCISZEK KASPRZYKOWSKI,[a] ZBIGNIEW GRZONKA,[a] JERZY CIARKOWSKI[a] and JACEK WÓJCIK[b]*

[a] Faculty of Chemistry, University of Gdańsk, Sobieskiego 18, PL-80-952 Gdańsk, Poland
[b] Laboratory of Biological NMR, Institute of Biochemistry and Biophysics, PAS, Pawińskiego 5a, PL-02-106 Warszawa, Poland

Received 16 October 2002
Accepted 4 March 2002

Abstract: Solution structures of two analogues of vasopressin with an amino acid sequence of *c*[Mpa^1-Tyr^2-Phe^3-Gln^4-Asn^5-Cys^6]-Xaa^7-Arg^8-Gly^9-NH$_2$ (Xaa = Sar [**I**] or MeAla [**II**]) were established using ROE and the $^3J_{HNH\alpha}$ couplings. Each of the peptides was found to exist in two stable isomers, pertaining to the *cis* or *trans* status of the Cys^6-Xaa^7 peptide bond, thus giving rise to four study objects.

Two methods for studies of the conformational properties of the structures were compared. In the first, the algorithm consisted of three steps: (i) An Electrostatically Driven Monte-Carlo (EDMC) search for low-energy conformations. (ii) Simulations of the NOESY spectra and the vicinal couplings for these conformations. (iii) Determination of the statistical weights of the conformations with the ANALYZE package, so as to meet the best fit of the averaged NOE intensities and couplings to the experimental data. In the second method, the distance constraints and the torsion angles were used as the usual constraints in the Distance Geometry and Simulated Annealing algorithms. The flexibility of the pressin ring and the *C*-terminus was characterized by a large number of families of conformations. The presence of the β-turn at position 4,5 was confirmed for all low energy structures found. The use of the EDMC method for the elaboration of the NMR data for small flexible peptides yielded an adequate description of their conformational diversity and is the method of choice for the analysis of their solution structures.

Keywords: vasopressin; [Sar^7]desaminoAVP; [MeAla^7]desaminoAVP; NMR spectroscopy; conformational studies; EDMC

Abbreviations: 2D, two-dimensional; AVP, [Arg^8]vasopressin; dAVP, desamino-AVP; DG, distance geometry; DMSO, dimethyl sulphoxide; DSS, 2,2-dimethyl-2-silapentane-sulphonic acid; ECEPPAK, a program for global conformational analysis of peptides; ECEPP/3, empirical conformational energy program for peptides; EDMC, electrostatically driven Monte Carlo; gHSQC, gradient heteronuclear single quantum coherence spectroscopy; HCTHMQC, pure phase homonuclear *J*-modulated heteronuclear multiple quantum coherence spectroscopy; MD, molecular dynamics; MORASS, multiple Overhauser relaxation analysis and simulation; SA, simulated annealing; Sar, sarcosine; SRFOPT, a model of fitting to small-molecule free energy hydration with atomic solvation parameters optimized using non-peptide thermodynamic data.

*Correspondence to: Dr Jacek Wójcik, Laboratory of Biological NMR, Institute of Biochemistry and Biophysics, PAS, Pawińskiego 5a, PL-02-106 Warszawa, Poland; e-mail: jacekw@poczta.ibb.waw.pl
Contract/grant sponsor: State Committee for Scientific Research, Poland; Contract/grant numbers: E-35/SPUB/P04/206/97; DS/8374-4-0138-1; 6P04A 024 17.

INTRODUCTION

The endogenous nonapeptide arginine vasopressin (c[CYFQNC]PRG-NH_2, AVP) is a hormone with a broad spectrum of functions. It controls urine concentration [1] and the blood pressure [2,3]. It is responsible for the stimulation of adrenocorticotropin secretion [4] and for the stability of the body temperature [5]. It influences some human behavioural [6] and sexual reactions [7]. This hormone also causes non-opioid anti-pain effects [8] and drug addiction [9]. It is thought that vasopressin may influence the higher functions of memorizing and learning [10].

AVP, together with its close homologue oxytocin (c[CYIQNC]PLG-NH_2, OT), are synthesized as precursor proteins in the neurophysis, from where they are transported to the posterior lobe of the pituitary and released into the blood [11]. Both nonapeptides consist of 20-membered rings, ensuing from the (1–6) disulphide, and the tripeptide amide *C*-terminal tail.

Much attention has been paid to the understanding of the relationship between the structure and biological activity of AVP. The structures of AVP and its analogues were studied using NMR and theoretical methods. Conformational analysis of AVP in DMSO using NMR and MD [12] revealed the presence of a well-defined β-turn involving residues from Tyr^2 to Asn^5. In addition the AVP molecule appeared to be very flexible in DMSO solution. The same conclusion resulted from the NMR investigations undertaken for native AVP in aqueous solution [13–15]. The structure could not be unequivocally defined since AVP molecules probe a large number of conformations. These findings corroborate earlier CD investigations of AVP in water [16]. Theoretical calculations of AVP in a vacuum [17] showed the existence of an equilibrium between 3,4 and 4,5 β-turns. The same β-turns were observed in the crystal structure of pressinoic acid [18]. Recently, models of AVP complexed to its V_{1a} and V_2 receptors were created using molecular modelling [19–21]. According to this model the pressin ring interacts with helices of the receptor and with extracellular loops while the *C*-terminal sticks out of the receptor and possesses a lot of freedom.

The combined NMR/MD method was applied for the conformational characteristics of several AVP analogues including [Mca^1]AVP, [Mca^1, Sar^7]AVP and [Mca^1, D-Phe^2, Sar^7]AVP [12]. In general each peptide showed structural changes at its mutation sites but the characteristic β-turn from Tyr^2 to Asn^5 was present in each conformation found. Furthermore, the agonists with Sar^7 reveal the presence of the additional conformers resulting from the *cis-trans* isomerization of the Cys^6-Sar^7 peptide bond.

Also, the conformational analysis with NMR of [AVP]CH_2 in DMSO [22] indicated a Tyr^2-Asn^5 β-turn of type I. The structure of 1-desamino-[D-Arg^8]VP (dAVP) found with NMR in water [23] and with MD in TFE [30,31] possesses the reverse γ-turn at Gln^4. Residues 1 and 2, the disulphide bridge and acyclic part of the peptide were found to be very flexible. The backbone of residues 4–6 fits well to the structure of pressinoic acid [18]. Additionally, conformation of the backbone from residues 2 to 6 conforms to the structure of oxytocin complexed to neurophysin II [24]. The structure of dAVP in TFE [25,26] is well defined. The first seven residues form a short distorted β-sheet with Tyr^2-Phe^3 in one and Cys^6-Pro^7 in the second thread linked with a Gln^4–Asn^5 β-turn of type I. The other β-turn is formed by residues Cys^6–Gly^9. This turn is of type II and is distorted. The crystal structure of pressinoic acid [18] contains two β-turns: 4,5 of type I and 3,4 of type II'. This structure also possesses a hydrogen bond between the H^N protons of the side chain of Gln^5 and the nitrogen atom of Tyr^2. The 3,4 β-turn was found for peptides [des-Gly^9]AVP [27] and LVP [28]. The 1–2 and 5–6 fragments of the backbone were found in the extended conformation. [Cpp^1, Sar^7]AVP in DMSO [29] proved to be flexible with 3,4 β-turns of various types. Gly-LVP in DMSO [30] exists with a γ-turn at Gln^4 while Gly-Gly-Gly-LVP gains a lot of flexibility in aqueous solution [31].

The NMR spectra of most analogues [29] of AVP with Sar^7 and analogues of oxytocin [32] with Sar^7 or $MeAla^7$ indicate the presence of two slowly interconverting conformers, which are the *cis-trans* isomers about the peptide bond between residues 6 and 7. When neurophysin is added to a solution of [Sar^7]oxytocin or [$NMeAla^7$]oxytocin the proportion of the minor conformer remains constant, indicating that *cis* and *trans* conformers are equally tightly bound to the protein [32].

Several papers reported the biological and structural effects of the replacement of the residue at position 7 in AVP. When this residue was replaced with 3,4-dehydroproline the biological activity of the analogue became high [33]. However, replacement with D-proline, glycine [34] or valine yielded compounds of low activity. Similarly, replacement of Lys^7

in arginine-vasopressin decreased the peptide activity [34]. The antidiuretic/pressor activity for [Mpa^1, Gly^7]AVP and [Gly^7]AVP is ca. 10 000 and 800 times, respectively, higher that of the parent hormone [36]. It can be concluded that substitution in position 7 of AVP and deamination of residue 1 leads to compounds with high antidiuretic/pressor selectivity. Some hope was offered by the high selectivity obtained for the hormone analogues, namely oxytocin having Gly at position 7 [37] and Sar^7 and NMeAla^7 oxytocin analogues [38].

The search for analogues of this hormone with increased activity and selectivity based on a better understanding of the structure–function relationship continues. The results obtained for the oxytocin analogues guided us to make the same modifications in arginine-vasopressin. It was shown that the MeAla^7, Sar^7 and Gly^7 vasopressin analogues exhibit higher antidiuretic selectivity than the wild peptide. In addition it was also shown that the antidiuretic relative activity (A/P ratio) is proportional to the degree of conformational freedom gained by the peptide at this position. However, this is accompanied by a decrease in the antidiuretic activity. The additional modification of these analogues, namely deamination at position 1, causes a further elevation of their selectivity with a decrease in their antidiuretic properties [27]. Since both deamination at position 1 and gaining of the conformational freedom at position 7 cause the same changes in the biological function of the peptide, one may assume a possible interaction of the *C*-terminal tripeptide with the *N*-terminal amine group in the wild peptide. It may also be assumed that the conformational freedom gained may itself sufficiently explain the observed increase in both peptides selectivity.

This assumption needs more support from NMR data. The solution NMR conformational studies of selective agonists of AVP, [Sar^7]desaminoAVP, **I** and [MeAla^7]desaminoAVP, **II** presented in this work were expected to supply additional arguments. In order to describe the flexibility of the cyclic peptide in a more quantitative way the promising method proposed by Liwo and co-workers [39,40] was applied in this study.

MATERIALS AND METHODS

NMR Experiment

The peptides were synthesized by the solid-phase technique and purified by reversed phase HPLC as described [41]. For NMR measurements the peptides were dissolved in a mixture of H_2O (DDI) and D_2O (99.8% isotopic purity, Dr Glaser, AG Basel) at a ratio of 10/1. The peptide concentration was 25 mM at a final pH of 4.0 and 5.1 for [Sar^7]dAVP, **I** and [MeAla^7]dAVP, **II**, respectively. NMR spectra of both analogues were measured at 25 °C with a UNITY500plus (Varian) spectrometer equipped with a Performa II gradient generator unit, WFG, Ultrashims, high stability temperature unit and a 5 mm $^1H\{^{13}C/^{15}N\}$ PFG triple resonance inverse probe head.

All spectra were measured with a water signal pre-saturation pulse typically of 2 dB and 1.5 s. The 1D proton experiments were taken at 5° to 50 °C. 16 K Data points were collected and a spectral width of 6 kHz was used. The 2D experiments were measured using a proton spectral width of 4.5 kHz collecting 2 K data points. TOCSY [42] and ROESY [43,44] spectra were measured with 256 increments. A mixing time of 80 ms was used in TOCSY while 300 ms was used in ROESY measurements. $\{^1H/^{13}C\}$ gHSQC [45–47] experiments with gradients were performed in proton de-coupled mode with a carbon spectral width of 25 kHz and 256 increments. $\{^1H/^{15}N\}$gHSQC experiments with gradients were performed in proton de-coupled mode with a nitrogen spectral width of 2 kHz and 128 increments.

The spectra were calibrated against the TSP signal taking into account the temperature drift of the reference signal given by the equation $\delta_{TSP} = -0.005 - 0.002335 \times T$ [K] [48]. External reference signals were used for calibration of correlation spectra — DSS for the carbon axis in $\{^1H/^{13}C\}$ spectra and the NH_3 signal for the nitrogen axis in $\{^1H/^{15}N\}$ spectra.

All NMR data were processed and cross-peak volume calculations were performed with an XEASY program [49] on the SUN Ultrasparc workstation.

The assignment of the proton signals was made by means of the clean TOCSY spectra [42]. The peptide sequence was confirmed with 25 °C ROESY spectra [43,44]. The chemical shifts are shown in Tables 1 and 2. Vicinal couplings, $^3J_{HNH\alpha}$, were measured using the HCTHMQC [50] spectrum for [Sar^7]dAVP, **I** and ct-COSY-ACT spectrum [51] for [MeAla^7]dAVP, **II** (Tables 1, 2 and Figures 1, 2). Torsion angles were generated using the HABAS algorithm [52] of the DIANA package [53], on the basis of the Bystrov-Karplus [54] equation. Intensities of ROE signals (Figures 1 and 2) were estimated from the ROESY spectra of both analogues. The possible

Table 1 Proton Chemical Shifts [ppm] and Proton–Proton Vicinal Couplings [Hz] of the *trans* and *cis* Isomers (major and minor, respectively) of [Sar^7]dAVP, **I** in Water at 25 °C

Residue		Chemical shift						$^3J_{HNH\alpha}$	$-\Delta\delta/\Delta T$
		H^N	H^α	H^β	H^γ	H^δ	Others		
Mpa^1	*trans*	—	2.72; 2.93	2.10				—	—
	cis	—	2.61; 2.72	n. o.*				—	—
Tyr^2	*trans*	8.174	4.49	2.72; 2.92			$H_{2,6}$ 6.79; $H_{3,5}$ 6.98	7.4	9.0
	cis	8.16	4.48	2.74; 2.92			n. o.*	6.7	n. o.*
Phe^3	*trans*	7.75	4.63	3.36; 3.02			$H_{2,6}$ 7.27; $H_{3,4,5}$ 7.38	7.5	7.5
	cis	7.78	4.60	3.34; 3.00			n. o.*	6.1	7.5
Gln^4	*trans*	8.37	4.10	2.10	2.29		δ-NH_2 6.86; 7.50	4.8	10.1
	cis	8.31	4.09	2.07; 2.14	2.28		7.50	4.4	8.9
Asn^5	*trans*	8.22	4.66	2.82; 2.63			ε-NH_2 6.88; 7.58	7.7	6.7
	cis	8.18	n. o.*	n. o.*			n. o.*	7.8	7.9
Cys^6	*trans*	8.17	5.08	3.12; 2.93				7.2	9.7
	cis	8.24	4.92	3.03; 2.93				8.0	8.8
Sar^7	*trans*	—	4.17; 4.06				N-C$\underline{H}_3$ 3.23	—	—
	cis	—	4.45; 4.28				3.16	—	—
Arg^8	*trans*	8.38	4.35	1.90; 1.77	1.65	3.20	ε-NH_2 7.18	7.0	11.6
	cis	8.59	4.38	1.90; 1.79	1.66	3.19	n. o.*	6.8	14.8
Gly^9	*trans*	8.48	3.92					—	9.8
	cis	8.55	3.89					—	12.0
C-end $N\underline{H}_2$	*trans*	(*E*) 7.45 (*Z*) 7.07						—	—

The last column contains the amide proton temperature coefficients [ppb/K].
* not observed.

Table 2 Proton Chemical Shifts [ppm] and Proton–Proton Vicinal Couplings [Hz] of the *trans* and *cis* isomers (major and minor, respectively) of [MeAla^7]dAVP, **II** in Water at 25 °C

Residue		Chemical shift						$^3J_{HNH\alpha}$	$-\Delta\delta\Delta T$
		H^N	H^α	H^β	H^γ	H^δ	Others		
Mpa^1	*trans*	—	2.96	3.15, 2.67				—	—
	cis	—	n. o.*	n. o.*				—	—
Tyr^2	*trans*	8.21	4.58	2.99, 2.78			$H_{2,6}$ 7.04; $H_{3,5}$ 6.84	7.6	4.8
	cis	n. o.*	n. o.*	n. o.*			n. o.*	7.7	n. o.*
Phe^3	*trans*	7.81	4.71	3.39, 3.07			$H_{2,6}$ 7.31; $H_{3,5}$ 7.46; H_4 7.40	8.0	2.5
	cis	7.67	4.74	3.37, 3.06			n. o.*	7.5	2.8
Gln^4	*trans*	8.41	4.15	2.13	2.33		δ-NH_2 7.54; 6.91	5.2	6.2
	cis	8.27	n. o.*	2.58	n. o.*		7.35	7.0	5.5
Asn^5	*trans*	8.28	4.75	2.87			ε-NH_2 7.62; 6.93	8.0	2.0
	cis	8.42	4.65	2.90			7.07	7.4	3.6
Cys^6	*trans*	8.19	5.05	3.13, 2.99				7.5	3.9
	cis	8.14	5.11	3.04				6.9	1.6
MeAla^7	*trans*	—	5.08	1.45			N-C$\underline{H}_3$ 2.86	—	—
	cis	—	5.08	1.55			2.85	—	—
Arg^8	*trans*	8.26	4.37	1.93, 1.81	1.67	3.26	ε-NH_2-7.24	6.9	4.6
	cis	8.43	4.42	1.94, 1.86	1.66	3.23	n. o.*	8.4	3.0
Gly^9	*trans*	8.48	3.97					—	4.4
	cis	8.53	3.96					—	4.8

The last column contains the amide proton temperature coefficients [ppb/K].
* not observed.

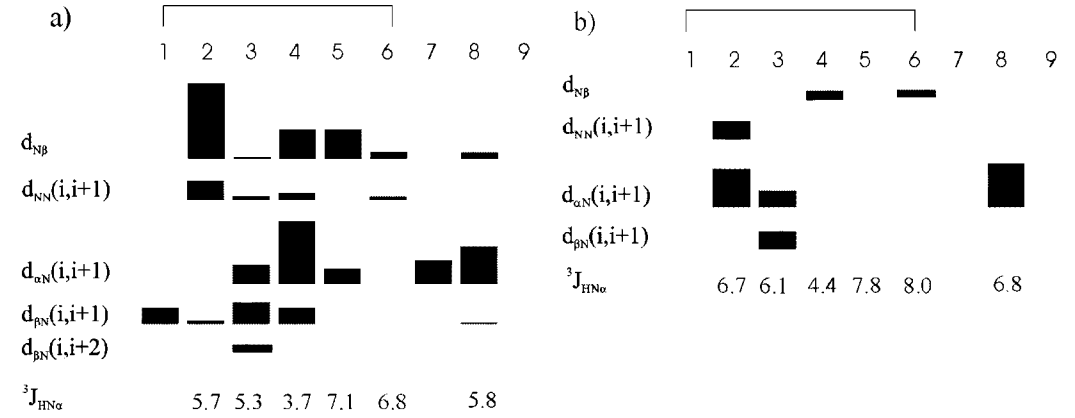

Figure 1 The integral intensities of off-diagonal signals in ROESY spectra and vicinal couplings ($^3J_{HNH\alpha}$) of [Sar^7]dAVP, **I** in water solution at 25 °C. (a) *trans* isomer; (b) *cis* isomer.

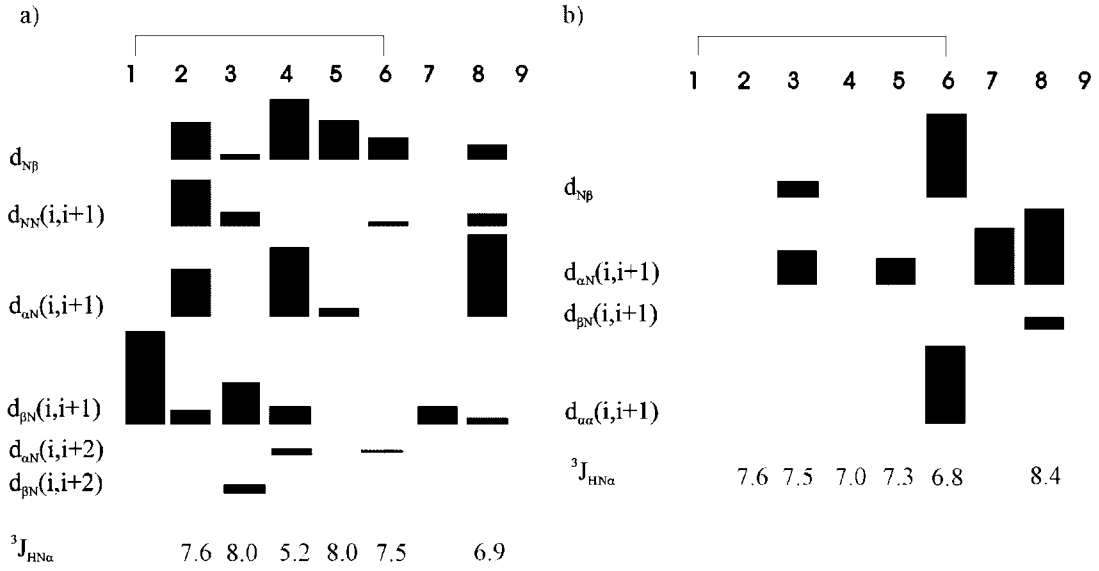

Figure 2 The integral intensities of off-diagonal signals in ROESY spectra and vicinal couplings ($^3J_{HNH\alpha}$) of [MeAla^7]dAVP, **II** in water solution at 25 °C. (a) *trans* isomer; (b) *cis* isomer.

exchange cross-peaks do not influence significantly the ROESY spectra since for the peptides studied the estimated maximal rate of chemical exchange ($k < 1\ s^{-1}$) was at least two times lower than the estimated rate of relaxation ($\rho_1 \approx 2.5\ s^{-1}$).

Inter-proton distances were generated using the CALIBA algorithm [55] of the DIANA package and calibrated against methylene protons. The numbers of ROE contacts obtained from the ROESY spectra, the numbers of important inter-proton distances and the torsion angles generated with DIANA packages (CALIBA and HABAS) are listed in Table 3. Temperature coefficients of the amide protons were estimated from temperature 1D spectra (Tables 1 and 2).

Conformational Calculations

The three-dimensional solution structures of both peptides were determined using two approaches:

1. Global conformational search of the peptide studied using the EDMC method with the ECEPP/3 force field and subsequent calculation of statistical weights of the obtained conformations by fitting the theoretical NOE effects and vicinal couplings $^3J_{HNH\alpha}$ to the experimental ones.
2. Using the restrained molecular dynamics SA, Simulated Annealing, protocol to obtain conformations that satisfy experimental data.

Table 3 Number of ROE Contacts Measured, Number of Structurally Important Interproton Distances Generated with the CALIBA Algorithm and Number of Torsional Angles Generated with the Program HABAS

Peptide	[Sar^7]dAVP, **I**		[MeAla^7]dAVP, **II**	
Isomer	*trans*	*cis*	*trans*	*cis*
ROE	102	29	133	34
CALIBA	73	26	96	34
HABAS	31	32	30	26

In the first method, a recently developed algorithm [39] was applied that allows the interpretation of the results obtained in terms of the multiconformational equilibrium of the peptide studied. In the first stage, all low-energy conformations were found by extensive global conformational analysis using the EDMC [56] method with the ECEPP/3 [57] force field. Then NOE intensities and vicinal couplings $^3J_{HNH\alpha}$ for each conformation were calculated. Finally, the statistical weights of these conformations by means of a non-linear least-squares procedure were determined, in order to obtain the best fit of calculated NOE intensities and vicinal couplings $^3J_{HNH\alpha}$ to the experimental NMR data. In the second method, a classical approach was applied that uses distance geometry and restrained molecular dynamics (with inter-proton distances calculated from NOE intensities and torsion angles calculated from vicinal couplings) to obtain conformations that satisfy experimental data. In the X-PLOR [58] calculations the standard implemented DG and SA protocols were used.

EDMC and ANALYZE Calculations

The search of the conformational space of the peptides studied was performed by the Electrostatically Driven Monte Carlo method (EDMC) [56]. Conformational energy was evaluated using the ECEPP/3 [56] force field, which assumes rigid valence geometry. According to the NMR data, the chirality of all C^α atoms (except that of the Sar residue) was fixed to the L configuration. The force field included hydration contribution, which was calculated using the SRFOPT surface-solvation method of Vila *et al.* [59] with original parameters. A dielectric constant, $\varepsilon = 2$, was used in the calculations according to the recommendation of the authors of the ECEPP/3 force field [56]. The temperature parameter in EDMC simulations was 1000 K, which corresponded to a reasonable acceptance rate of 20%–30%. The software used was the ECEPPAK global conformational analysis package [60]. Finally, 3000 energy-minimized conformations were accepted, subsequently clustered using the minimum-variance algorithm [61]. The root mean square deviation (RMSD) between heavy atoms at optimal superposition was taken as a measure of the distance between conformations, and a cut-off value of 0.1 Å was used to separate the families to afford 964 families of conformations for [Sar^7]dAVP, **I** and 420 for [MeAla^7]dAVP, **II**.

In the next step the NOE intensities and the $^3J_{HNH\alpha}$ vicinal couplings for the lowest energy conformations from each family were calculated. The intensities of NOE signals were computed by solving the system of the Bloch differential equations [62] applying the MORASS2.1 program [63,64]. The vicinal $^3J_{HNH\alpha}$ couplings of low-energy conformations were calculated from the empirical Bystrov-Karplus relationship [54]. Based on the sets of measured and theoretically calculated observables, the statistical weights of the conformations were fitted to obtain the best agreement between the theoretical and experimental value, using the algorithm developed by Groth *et al.* [40]. The NOE effects were generated using a correlation time of 0.45 ns [28,65] and a mixing time of 300 ms. The statistical weight for the coupling term was set to 0.01, and the Marquardt convergence criterion equal to 10^{-5} was used. Calculations were carried on an IBM 9076 Scalable POWER Parallel System (SP2) and on a Sun Enterprise 1000 computer.

Conformations with statistical weights exceeding 1% for [Sar^7]dAVP, **I** and 2% for [MeAla^7]dAVP, **II** were used in further comparative analysis. These cut-offs had to be applied since there were so many diverse conformations with very low weights that any comprehensible analysis would be impossible. Refitting based only on the conformations with higher populations did not change the agreement between experimental and calculated NOE intensities and $^3J_{HNH\alpha}$ values by more than 10%. It should be realized, however, that the selected representative conformations do not constitute the entire conformational ensemble.

X-PLOR Distance Geometry and Simulated Annealing Simulations

In the second approach the structure of each peptide was produced using distance and torsion angle

constraints. The standard modules of the X-PLOR program [42] were used. The SA algorithm was used for both peptides. The calculations were carried using the CHARMM force field [66] *in vacuo* starting from a random structure. Electrostatic interactions and energy of hydrogen bonds were not directly included and van der Waals interactions were described with the simplified potential function. According to the NMR data, the inter-proton distances ($f = 50$ kcal/(mol$\times$ Å^2), torsion angles ($f = 5$ kcal/(mol $\times$ rad^2) and geometry of the peptide group (all *trans*) ($f = 500$ kcal/mol $\times$ rad^2) were kept fixed. Also the chirality of all C$^\alpha$ atoms, except for the glycine residues was fixed to L ($f =$ 500 kcal/mol $\times$ rad^2). For both molecules 300 cycles of SA were carried out. Each cycle included 27 000 iterations of 80 ps with the 3 fs steps. The molecule was heated at 1000 K for 50 ps and annealed at 100 K for 29 ps. In the last 200 iterations (1 ps) energy minimization with the use of the Powell algorithm [68] was performed. During SA refinement the molecule was slowly cooled from 1000 K to 100 K for 30 ps. Finally, 300 energy-minimized conformations were obtained. The set of the final conformations was clustered (using the minimal-tree algorithm).

The RMSD between heavy atoms at optimum superposition was taken as a measure of the distance between conformations, and the cut-off value of 2.2 Å was used to separate the families. In a further analysis seven families of conformations for [Sar^7]dAVP, **I** and eight families of conformations for [MeAla^7]dAVP, **II** were considered. Molecular structures were drawn and analysed with the graphic program MOLMOL [68].

RESULTS AND DISCUSSION

NMR Results

In this work an NMR conformational study of two non-selective agonists of AVP, [Sar^7]dAVP, **I** and [MeAla^7]dAVP, **II** in aqueous solution is presented. Inspection of the 1D and 2D NMR spectra revealed that both peptides exist in two slowly interconverting isomers. In the ROESY spectra of both peptides the ROE cross-peaks between H$^\alpha$ protons of residues 6 and 7 were observed for less populated isomers thus confirming the *cis* configuration on the peptide bond that links these residues. For more populated isomers the presence of the ROE cross-peaks between the H$^\alpha$ proton of residue 6 and the N-CH$_3$ protons of residue 7 indicates the *trans* configuration on that peptide bond. In addition, the presence of chemical exchange cross-peaks in the ROESY spectrum for H$^\alpha$ protons of Xaa^7 residue indicates its *cis*/*trans* isomerization. An elevation of temperature slightly increases the population of the *cis* isomer from 30% at 5 °C to 40% at 40 °C for [Sar^7]dAVP, **I** and from 20% at 10 °C to 40% at 50 °C for [MeAla^7]dAVP, **II**.

Figures 1(a) and 1(b) summarize the ROE patterns and vicinal couplings, $^3J_{HNH\alpha}$, obtained for [Sar^7]dAVP, **I**. In the case of the *trans* isomer [Figure 1(a)] the H^N(2) - H^N(3), H^N(3) - H^N(4) and H^N(4) - H^N(5) ROE cross-peaks indicate the presence of the β-turn at position 2,3 or 3,4. The presence of the H$^\alpha$(i) - H^N(i+1) and H$^\beta$(i) - H^N(i+1) cross-peaks suggests that the β-turn at position 3,4 is populated. The small value of the $^3J_{HNH\alpha}$ coupling of residue 4 (3.8 Hz) and the higher value measured for residue 5 (7.0 Hz) suggest the presence of a β-turn at 4,5 position. For the *cis* isomer [Figure 1(b)] of this analogue the H^N(2) - H^N(3) and the H$^\alpha$(2) - H^N(3) and H$^\alpha$(3)-H^N(4) ROE cross-peaks suggest the presence of a β-turn at position 2,3. No changes in the coupling values were observed in comparison with the *trans* isomer. Large values of the temperature coefficients of the H^N protons of [Sar^7]dAVP, **I** for both isomers (Table 1) suggest the lack of hydrogen bonds. The curves $\Delta\delta/\Delta T$ are linear for all the isomers within the tested range of temperature.

Figures 2(a) and 2(b) show the ROE effects patterns, vicinal couplings values, $^3J_{HNH\alpha}$, and temperature coefficients of amide signals obtained for [MeAla^7]dAVP, **II**. In the case of the *trans* isomer [Figure 2(a)] the ROE cross-peaks: H^N(2) - H^N(3), H^N(3) - H^N(4) and H$^\alpha$(2) - H^N(3) suggest the presence of the β-turn at position 2,3; the presence of the cross-peaks: H$^\alpha$(4)- H^N(5), H$^\alpha$(5) - H^N(6) and H$^\alpha$(4) - H^N(6) suggest a β-turn at position 4,5. Additional cross-peaks: H$^\alpha$(5)- N(CH$_3$)(7) and H^N(6) - N(CH$_3$)(7) confirm the β-turn at position 5,6. The small value of the $^3J_{HNH\alpha}$ coupling of residue 4 (5.2 Hz) and the higher value measured for residue 5 (8.0 Hz) suggest the presence of a β-turn at the 4,5 position. The small value of the temperature coefficient of the H^N of Phe^3 may be caused by the hydrogen bonding of this proton to the oxygen atom of the carbonyl group of Cys^6, (β-turn) or to the oxygen atom of the carbonyl group of Mpa^1 (γ-turn). The small value of the coefficient was also observed for the signal of the proton H^N of Asn^5, which may form a hydrogen bond to the oxygen atom of carbonyl group of Tyr^2 (β-turn) or Phe^3 (γ-turn). This proton may be involved in the hydrogen bond with other groups.

For the *cis* isomer of [MeAla^7]dAVP, **II** [Figure 2(b)] a small number of ROE cross-peaks was observed. The H^N - H^N cross-peaks were lacking. The presence of cross-peaks of the H^α(i) - H^N(i+1) type between the pairs of residues 3,4; 5,6; 7,8 and 8,9 may confirm the presence of the corresponding β-turns. However, the values of $^3J_{HNH\alpha}$ couplings are rather high and do not suggest the occurrence of any type of β-turn. The small value of the temperature coefficient of the H^N of Cys^6 of the *cis* isomer may be caused by hydrogen bonding of this proton to the oxygen atom of the carbonyl group of Phe^3 residue involved in the β-turn of the 4,5-type or by hydrogen bonding to the oxygen of the side chain carbonyl group of Gln^4 in the γ-turn. This proton may be also involved in the hydrogen bond with other groups. The small value of the temperature coefficient was also observed for the signal of the proton H^N of Phe. The proton may form a hydrogen bond to the oxygen atom of the carbonyl group of Cys^6 (β-turn) or Mpa^1 (γ-turn). Also the coefficient of the H^N proton of Arg^8 residue is small. This proton may form a hydrogen bond to the oxygen atom of the carbonyl group of Asn^5 (β-turn) or Cys^6 (γ-turn).

Discussion of the Results Obtained with the ANALYZE Program

The statistical weights of the β-turns obtained in the conformers of both analyzed compounds **I** and **II** are given in Tables 4 and 5. The Lewis criterion [68] was used to evaluate the position and the type of β-turn for each accepted conformation. The measured and computed values of vicinal couplings of both analogues, $^3J_{HNH\alpha}$, and standard deviations for couplings and ROE peak volume are shown in Table 6. It may be seen that the standard deviations are generally smaller than 1.0, except those for the [MeAla^7]dAVP, **II** *trans* isomer. This means an agreement between the experimental data and the obtained structures of both analogues.

The conformers found for the *trans* isomer of [Sar^7]dAVP, **I** [Figure 3(a)] might be separated in two groups. The first group contains the conformations with two β-turns at positions 2,3 and 3,4, both of type I. The second group is formed by conformers with a β-turn at position 4,5 of type I. The obtained conformers create a γ-turn involving positions Asn^5, Arg^8 and Gly^9. The majority of calculated conformers form a hydrogen bond between the H^N proton of Arg^8 and the carbonyl group of Cys^6. The *cis* isomer [Figure 3(b)] exists mainly in conformations with consecutive β-turns at positions 4,5 (type I); 6,7 (type IV) and 7,8 (type IV or II'). The large conformational freedom at the *C*-terminus (residues 7–9) causes a small number of ROE contacts measured for these residues. The conformers of the *cis* isomer contain a γ-turn at positions Asn^5 and Gln^4. Three obtained conformers form hydrogen bonds between the H^N protons of the *C*-terminal amide group and the carbonyl group of Asn^5. This hydrogen bond stabilizes the β-turn at position 7,8.

The conformations of the pressin rings of both isomers of the highest value statistical weights [Figure 4(a)] are very similar, with $RMSD_{1-6}$ for C^α atoms of 0.705 Å. These conformations exhibit a significant structure difference at the *C*-terminus that is caused by the *cis* or *trans* arrangement on the 6,7 peptide bond. The *C*-terminal tripeptide of both isomers is oriented in the opposite direction.

The conformers found for the *trans* isomer of [MeAla^7]dAVP, **II** [Figure 3(c)] contains mainly β-turns at position 4,5 of type I and II. Additionally, conformers with β-turns of type VI were observed at position 5,6. The majority of calculated conformers contain a γ-turn at positions Asn^5, Gln^4, Arg^8 and Gly^9. The conformations of the *cis* isomer [Figure 3(d)] may be separated in two groups. The conformations of the first group contain a β-turn at position 2,3 of type III followed by a β-turn of type III or IV at position 3,4. In the second group conformations with a β-turn of type I at position 4,5 are included. All calculated conformers create a γ-turn at Gly^9. The obtained conformers of the two isomers form hydrogen bonds, which are in very good agreement with experimental data. They stabilize β-turns at positions 1,2; 3,4; 4,5; 6,7 and γ-turns in the region Phe^3-Asn^5.

The comparison of the pressin ring of conformations with the highest statistical weights of *trans* isomers of both peptides [Figure 4(c)] reveals again a rather small structural difference within this part of the molecule with $RMSD_{1-6}$ of 0.080 Å for C^α atoms. For the *cis* isomers [Figure 4(d)] a larger value of $RMSD_{1-6}$ was found of 1.747 Å (for C^α atoms), but this result should be treated with lower confidence since for the *cis* isomer the number of measured ROE contacts was rather small. It means that the conformations of the pressin ring do not differ significantly upon substitution at position 7 of dAVP with Sar, **I** or NMeAla, **II**.

Discussion of the Results Obtained with the X-PLOR

The calculations with the X-PLOR program were performed for the *trans* isomers only of both **I**

Table 4 Statistical Weights of the Lowest Energy Conformations (with weights above 1%) of the *trans* and *cis* isomers of [Sar^7]dAVP, **I** Analogue in Water at 25 °C Obtained with EDMC and ANALYZE

trans isomer				*cis* isomer			
Positions and types of turns	H-bonds	Number of conformation; geometry of SS-bond	Population (%)	Positions and types of turns	H-bonds	Number of conformation; geometry of SS-bond	Population (%)
4,5 β I 5 γ^*, 9γ^*	NH^8-CO^6	143 R	2.9	4,5; I 6,7; IV 7,8; I 5 γ^*, 9γ	NH^6-CO^4	010 R	1.5
4,5 β III	NH^8-CO^6	160 R	1.0	4,5; I 6,7; II 7,8; I 5 γ^*,9γ	NH^9-CO^5	026 L	1.2
4,5 β I 5 γ^*, 8γ^*, 9γ	NH^8-CO^6	161 R	13.0	4,5; I 5 γ^*	NH^6-CO^4	049 L	1.4
2,3 β I 3,4 β I 9γ^*	NH^8-CO^6	238 L	1.9	4,5; I 6,7; IV 7,8; IV	—	102 R	6.6
2,3 β I 3,4 β III'	NH^{2,3,5} – δCO^5 NH^8-CO^6	239 R	1.1	4,5; I 6,7; IV 7,8; III 9γ	NH^{2,3}-CO^9 NH^9-CO^5	212 R	2.3
2,3 β I 4,5 β III	NH^8-CO^6	259 L	1.5	4,5; I	—	413 R	1.2
4,5 β III	—	282 L	1.1	2,3; III 3,4; IV 4,5; IV 6,7; III 7,8; IV 5 γ^*, 9γ	NH^2-CO^7 NH^9-CO^5	414 L	1.3
2,3 β I 4,5 β III 9γ	NH^8-CO^6	358 L	1.4				
4,5 β I 9γ^*	—	428 L	9.1				
2,3 β I 7,8 β III	—	430 L	1.6				
4,5 β I 9γ^*	NH^8-CO^6	431 L	3.0				
2,3 β I 3,4 β III'	NH^{2,3} – δCO^5	432 L	3.6				
2,3 β I 3,4 β III' 5,6 β IV 8γ^*	NH^{2,3} – δCO^5	433 L	1.4				
4,5 β I 5 γ^*, 9γ^*	—	450 L	3.6				

γ^*, inverse gamma turn.

Table 5 Statistical Weights of the Lowest Energy Conformations (with weights above 2%) of the *trans* and *cis* isomers of [MeAla^7]dAVP, **II** Analogue in Water at 25 °C Obtained with EDMC and ANALYZE

trans isomer				*cis* isomer			
Positions and types of turns	H-bonds	Conformation number geometry of SS bond	Pop. (%)	Positions and types of turns	H-bonds	Conformation number geometry of SS-bond	Pop. (%)
4,5 β III 5,6 β VI	NH^3-CO^6 NH^{6,8}-CO^3	148 R	2.4	2,3 β III 3,4 β IV 5,6 β VI 6,7 β IV 9 γ	—	489 L	2.8
2,3 β III 4,5 β III 5,6 β VI 6,7 β IV 8 γ^*	NH^6-CO^3 NH^8 – δCO^5	202 R	7.8	4,5 β I 5,6 β VI 6,7 β IV 5 γ^*, 9 γ	NH^6-CO^4	526 R	2.9
— 4 γ^*	NH^5-CO^3	227 L	2.5	4,5 β III 5,6 β VI 6,7 β IV	NH^3-CO^6 NH^8-CO^3	512 R	5.7
4,5 β I 5 γ^*	—	256 L	5.7	4,5 β I 5,6 β VI 6,7 β IV 9 γ	NH^3-CO^6 NH^8-CO^4 NH^9-CO^4	030 R	2.7
3,4 β I 4,5 β IV 9 γ^*	NH^5-CO^2	290 L	5.7	2,3 β III 3,4 β IV 5,6 β VI 6,7 β IV 9 γ	NH^2 – δCO^5	210 L	7.4
4,5 β I 5 γ^*, 8 γ^*	—	308 L	3.4	2,3 β III 3,4 β III 6,7 β II	NH^8-CO^5	312 L	3.9
4,5 β I 6,7 β IV 5 γ^*	—	316 R	11. 8	2,3 β III 6,7 β IV 9 γ	NH^8 – δCO^5	342 L	4.2
4,5 β III 6,7 β IV 8 γ^*	—	342 R	2.0	2,3 β III 6,7 β IV 9 γ	NH^8 – δCO^5	357 R	3.1
4,5 β III 5,6 β VI 8 γ^*	NH^3-CO^6 NH^8-CO^3	350 L	3.1	2,3 β III 3,4 β IV 6,7 β IV	NH^2 – δCO^5	360 L	13.8
4,5 β I 5,6 β IV	NH^3-CO^6 NH^6-CO^3	355 L	3.7	2,3 β III 6,7 β IV 9 γ	NH^8 – δCO^5	442 R	4.6
— 5 γ^*	NH^5-CO^3	369 L	4.5	3,4 β III 4,5 β I 5,6 β VI 6,7 β IV	NH^5-CO^2 NH^9-CO^4	612 L	3.2
3,4 β III 6,7 β II 9 γ^*	NH^2-CO^5	371 R	2.6	2,3 β III 6,7 β IV 9 γ	NH^8 – δCO^5	634 R	3.1
4,5 β III 5,6 β VI 9 γ	NH^3-CO^6 NH^8-CO^3 NH^{10}-CO^8	374 L	10.7	2,3 β I 3,4 β III 6,7 β I	NH^2-CO^9 NH^3-CO^9 NH^9-CO^5	641 L	4.3

Table 5 (*Continued*)

trans isomer				*cis* isomer			
Positions and types of turns	H-bonds	Conformation number geometry of SS bond	Pop. (%)	Positions and types of turns	H-bonds	Conformation number geometry of SS-bond	Pop. (%)
				7,8 β IV 9 γ			
4,5 β I 5 γ^*, 9 γ^*	—	375 R	4.1	3,4 β IV 6,7 β IV 9 γ	NH^8 – δCO^5 NH^9 – δCO^5	740 L	30.6
4,5 β I 5 γ^*	—	415 L	19.4	2,3 β IV 6,7 β I	NH^9 – δCO^5	751 L	2.4

γ^*, inverse gamma turn.

Table 6 Measured and EDMC/ANALYZE Computed Values of the Vicinal Couplings, $^3J_{HNH\alpha}$ [Hz] of [Sar^7]dAVP, **I** and [MeAla^7]dAVP, **II**

Peptide	[Sar^7]dAVP, **I**		[MeAla^7]dAVP, **II**	
Residue	J_{calc}	J_{exp}	J_{calc}	J_{exp}
	trans isomer			
2	7.665	7.4	8.088	7.6
3	7.733	7.5	8.717	8.0
4	5.580	4.8	5.518	5.2
5	6.592	7.7	6.991	8.0
6	7.466	7.2	7.621	7.5
8	6.906	7.0	6.186	6.9
Sd[a]	0.5828		0.6318	
Sd[b]	0.7277		1.6825	
	cis isomer			
2	7.551	6.5	7.785	7.6
3	7.306	6.1	7.167	7.5
4	4.660	4.4	7.361	7.0
5	7.191	7.8	7.684	7.3
6	7.016	8.0	7.761	6.8
8	6.017	6.8	6.775	8.4
Sd[a]	0.8734		0.8150	
Sd[b]	0.1438		0.4352	

[a] Standard deviation in vicinal couplings.
[b] Standard deviation in ROE cross-peak volumes.

and **II**, since the number of restraints found for the minor *cis* isomers was too small. The lowest energy conformations of [Sar^7]dAVP, **I** possess a β-turn at positions 2,3; 3,4 and 4,5. All conformations have a β-turn of type III at position 4,5 [Figure 5(a), Table 7]. Three calculated conformers have a γ-turn at position Gly^9. Two obtained conformers form hydrogen bonds between δH^N protons of Asn^5 to the carbonyl group of Gln^4 and additionally H^N proton of Gln^4 to the hydroxyl group of OH^4.

The lowest energy conformations found for the [MeAla^7]dAVP, **II** peptide have consecutive β-turns of the type II' at position 3,4 and of type IV at position 4,5. The remaining conformations have β-turns at positions 3,4 and 4,5 [Figure 5(b), Table 7]. Most of the calculated conformers form a hydrogen bond with the H^N proton of Asn^5 to the carbonyl group of Phe^3. This hydrogen bond stabilizes the β-turn at position 4,5 in the fragment Phe^3-Cys^6.

The comparison of conformations of the pressin ring of *trans* isomers of both peptides obtained with the X-PLOR method [Figure 5(c)] reveals small structural differences with RMSD$_{1-6}$ of 1.954 Å for C$^\alpha$ atoms. It means that the substitution with Sar and MeAla at position 7 of dAVP did not change very much the conformation of the pressin ring.

Comparison of the Results Obtained with the ANALYZE and X-PLOR

The qualitative structural conclusions drawn for two isomers of both peptides from inspection of the NMR data have been confirmed using two calculation methods. This concerns mainly the β-turn locations. The obtained structures contain also many hydrogen bonds confirming the NMR data in respect of the donor locations. However, the acceptor location in most cases is not clear since there are many possible acceptors including the side chains of Tyr^2, Gln^4, Asn^5 or Arg^8.

The structures of the *trans* isomers obtained from calculations using the two methods differ in some way with the largest RMSD$_{1-6}$ of 2.182 Å and of

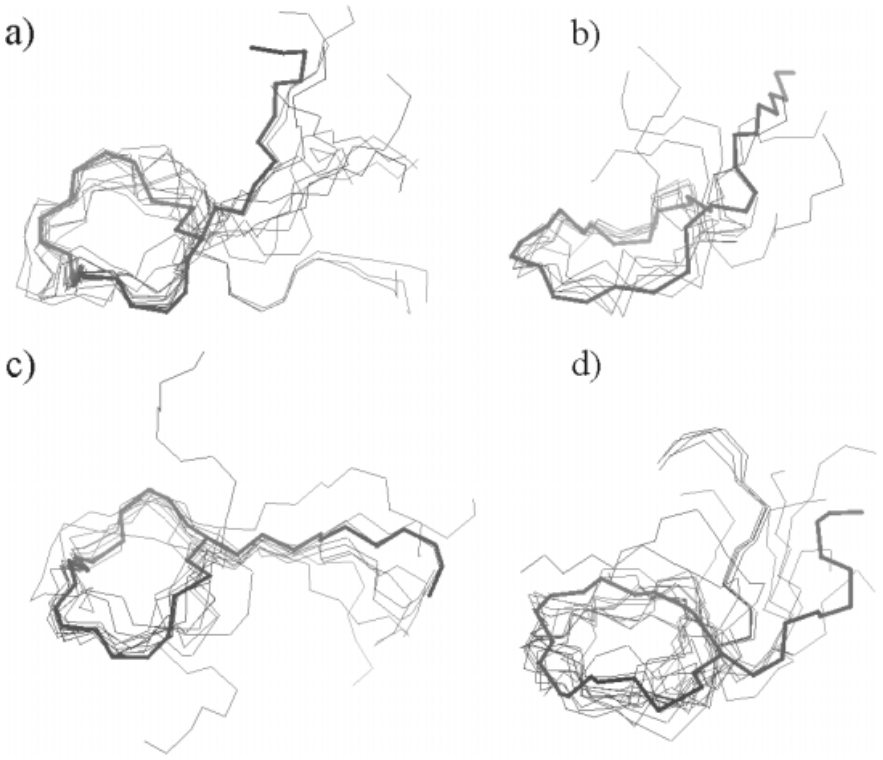

Figure 3 Superposition of the lowest energy conformations obtained with EDMC/ANALYZE; (a) *trans* isomer and (b) *cis* isomer of [Sar^7]dAVP, **I;** (c) *trans* isomer and (d) *cis* isomer of [MeAla^7]dAVP, **II**. RMSD$_{1-6}$ = 0.874; 0.552; 0.745 and 1.117 Å, respectively. For details see Tables 4 and 5. The bold line represents the backbone of the most populated conformation.

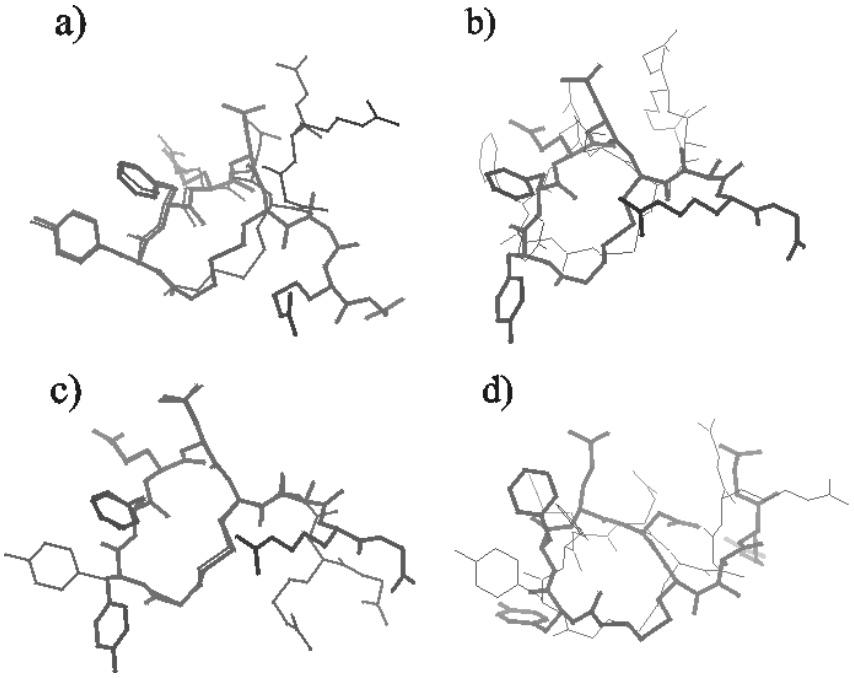

Figure 4 Comparison of the two isomers *cis* and *trans* of the lowest energy conformations obtained with EDMC /ANALYZE. (a) superposition of *cis* isomer (thick line) and *trans* (bold line) of **I**; (b) superposition of *cis* isomer (thick line) and *trans* (bold line) of **II**. Comparison of **I** and **II**. (c) superposition of *trans* isomer of **I** (thick line) and **II** (bold line); (d) superposition of *cis* isomer of **I** (thick line) and **II** (bold line). RMSD$_{1-6}$ = 0.705; 1.623; 0.080 and 1.747 Å, respectively.

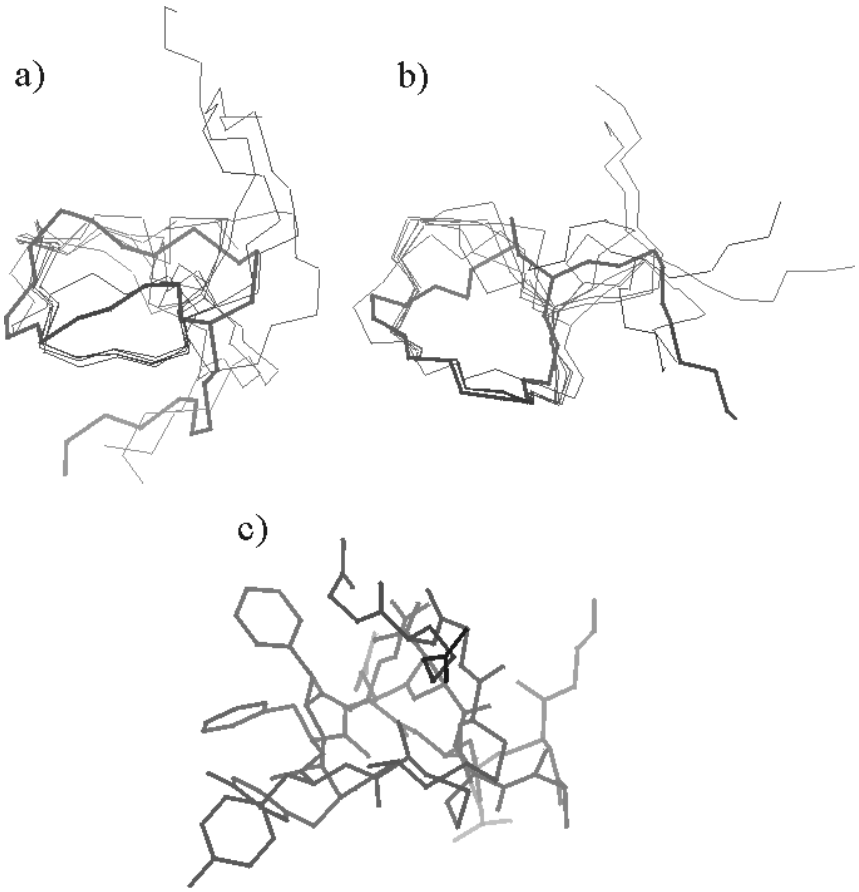

Figure 5 Superposition of the lowest energy conformations obtained with X-PLOR. (a) *trans* isomer of **I**; (b) *trans* isomer of **II.** The bold line represents backbone of the most populated conformation: (c) comparison of *trans* isomer of **I** (bold line) and **II** (thick line). $RMSD_{1-6}$ = 1.044; 0.559 and 1.954 Å, respectively. For details see Table 7.

3.492 Å found for the pressin ring of **I** and of **II**, respectively. For more details see Figures 6(a) and 6(b). Significant differences in the 3D structures were found also for the mobile residues from 7 to 9 at the *C*-terminus of the peptides. However, the overall structures are only moderately different. The observed differences resulted from the methods themselves, since the ANALYZE program uses parameterization for water as a solvent and the ECEPP/3 force-field uses charges while the X-PLOR calculations were carried in a vacuum with the CHARMM force-field lacking charges. In addition, in the ANALYZE calculations the mixing and the correlation time were included which is very important in the case of small and mobile peptides. On the other hand the X-PLOR program uses constraints generated with the program DIANA, originally dedicated and setup for the assignment of rather large proteins with little conformational freedom. Therefore, one may assume that the structures found with the ANALYZE method better describe the conformational behaviour of the peptides in solutions and that the estimated distribution of conformations fits better to the actual conformational equilibrium as well.

Comparison of our Results to those Previously Reported for Vasopressin

The NMR structure of AVP vasopressin analogues was reported by Schmidt *et al.* [12]. Yu *et al.* [28] published the structure of lysine-8 vasopressin. The presence of β-turns at position 3,4 in low energy conformations of the pressin ring was postulated earlier by many authors [10,70]. The exhaustive theoretical conformational analysis of the pressin ring was reported recently by Liwo *et al.* [39] For the cyclic part of arginine-8 vasopressin in aqueous solution the smallest value of RMSD was obtained by the authors for those families of conformations with a single β-turn at position 3,4 or 4,5. The

Table 7 Families of Low Energy X-PLOR conformations from Each Family of *trans* Isomers of [Sar^7]dAVP, **I** and [MeAla^7]dAVP, **II** in H_2O/D_2O at 25 °C

[Sar^7]dAVP, **I** *trans* isomer				[MeAla^7]dAVP, **II** *trans* isomer			
Positions and types of turns	H-bonds	Conformation number; geometry of SS bond	Number of conformations in each family cut = 2.2 Å	Positions and types of turns	H-bonds	Conformation number geometry of SS bond	Number of conformations in each family cut = 2.2 Å
2,3 β I 3,4 β VII 4,5 β VII 9γ	—	48 R	21	2,3 β IV 4,5 β IV 6,7 β II	NH^5-CO^3	113 R	276
2,3 β III 3,4 β VII 4,5 β VII 6,7 β VII 7,8 β IV	δNH^5-CO^4	238 R	154	3,4 β II' 4,5 β IV	NH^5-CO^3	46 R	16
4,5 β IV 9γ *	NH^4-OH^4	237 L	22	3,4 β II' 4,5 β IV 6,7 β II	NH^5-CO^3	285 R	3
4,5 β VII 7,8 β IV	—	145 R	66	3,4 β IV 4,5 β IV 6,7 β II	NH^5-CO^3	266 R	1
4,5 β VII	—	291 R	3	3,4 β II' 4,5 β IV	NH^5-CO^3	78 L	1
4,5 β VII	—	208 L	4				
4,5 βVII 9γ*	—	76 L	22	4,5 β IV	NH^5-CO^3	123 L	1
				3,4 β II' 4,5 β IV 5,6 β III 6,7 β I	NH^5-CO^3	157 L	1
				3,4 β II' 4,5 β IV	—	295 R	1

L, left-handed disulphide bridge; R, right-handed disulphide bridge; γ*, inverse gamma turn.

authors also found that the presence of the turn at position 2,3 was more characteristic for the pressin ring of oxytocin [39]. The tendency of the pressin ring to form β-turns at positions 2,3; 3,4 and 4,5 was confirmed in our investigation of vasopressin analogues lacking the *N*-terminal amino group and with proline-7 substituted with the residues offering more conformational freedom.

The conformations with one α-helix turn involving residues 3 to 5 were postulated among the lowest energy conformations of AVP [39]. This type of local structure is rather excluded in the peptides investigated in this work since for the residues 3 and 5 large values of couplings were measured and ROE cross-peaks typical of α-helix were lacking.

Biological Relevance of the Results

The molecular interaction models for AVP-V_{1a} (pressor) receptor, V_{1aR} [18] and for AVP-V_2 (antidiuretic) receptor, V_{2R} [20,21] have been proposed and

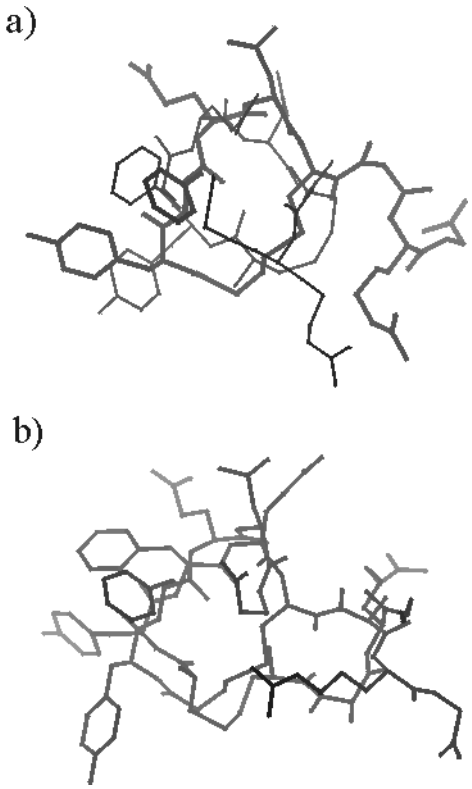

Figure 6 Comparison of the lowest energy peptide conformations obtained with X-PLOR (thick line) and EDMC/ANALYZE (bold line). (a) *trans* isomer of **I**; (b) *trans* isomer of **II**. $RMSD_{1-6} = 2.182$ and 3.492 Å, respectively.

described. Despite being quite speculative and different in detail, they have a few things in common. (i) Apart from details in molecular modelling procedures [18,20], both the V_{1a} and V_2 receptor models have been based on the common template, i.e. the low-resolution experimental model of a homologous bovine rhodopsin [71]. (ii) In both models, there have been several equivalent receptor residues recognized and experimentally confirmed [18] as those directly relevant to AVP affinity. (iii) Although different in detail (e.g. the pressin ring in V_{1aR} forms a pseudo β-sheet limited by the disulphide and Phe^3-Gln^4 turns, while in V_{2R} it forms a pseudo β-sheet limited by Tyr^2-Phe^3 and Asn^5-Cys^6 turns, respectively), both receptor-bound AVP models have a common feature. This feature consists of maximizing the polar backbone interactions of the pressin ring with the receptor pocket and is actually opposite to what is observed and actually expected in any solution conformation(s). On the other hand, such a maximization of the intermolecular pressin backbone–receptor pocket polar interactions is not a surprise if one considers that a typical receptor, being an integral membrane protein, is polar inside and hydrophobic outside its heptahelical transmembrane domain. In summary, although the receptor-bound AVP pressin ring adopts a β-sheet-like shape, most if not all its backbone peptide planes are turned away and roughly perpendicular to its averaged 'β-sheet' plane, thus arranging the pressin ring into a pseudo rather than a true β-sheet(see Figure 5). Simultaneously, this feature is unlikely to occur in solution conformations. Thus, in typical cases like these, despite cyclic constraints the biological relevance of solution conformations of flexible peptides may be questioned.

CONCLUSIONS

It appears that substitution of the proline residue at position 7 of vasopressin with sarcosine or *N*-methyl alanine accompanied by deamination of the *N*-terminus for the peptide gains more flexibility of the pressin ring. Calculation with the ANALYZE method reflects the flexibility of both peptides, **I** and **II**, much better than calculation using the X-PLOR program. Both methods yielded the structures of vasopressin analogues with a β-turn of type I or III at position 4,5. Several other turns were also found. A variation in temperature shifts the *trans - cis* equilibrium at position 7 towards the less populated *cis* isomer. It is clear that the increased flexibility and conformational diversity of peptides make tracing the *C*-end and *N*-end interference more difficult, if not impossible. Therefore, the observed increased selectivity of the analogues, [Sar^7]desamino- and [MeAla^7]desamino- vasopressin may be rationalized by their conformational freedom gained allowing tighter fitting to the receptor.

Acknowledgements

Professor H. Scheraga (Cornell University) is acknowledged for his kind permission for use of the ECEPPAK program and Professor A. Liwo, Dr S. Ołdziej and Dr C. Czaplewski (University of Gdańsk) are acknowledged for their kind permission for use of the ANALYZE program.

The use of the NMR facility of the Laboratory of Biological NMR, Institute of Biochemistry and Biophysics, Polish Academy of Sciences (partly supported by State Committee for Scientific Research, KBN, grant E-35/SPUB/P04/206/97) is gratefully acknowledged. The authors also acknowledge KBN

for grant DS/8374-4-0138-1. J.C. acknowledges KBN grant no. 6P04A 024 17. The calculations were carried out in the Academic Computer Centre (TASK) in Gdańsk, Poland, and Interdisciplinary Center for Mathematical Modelling (ICM) in Warsaw, Poland.

S.R-M. is a recipient of a fellowship from the Foundation for Polish Science.

REFERENCES

1. Bockaert J, Roy C, Rajerison R, Jard S. Specific binding of [3H]lysine-vasopressin to pig kidney plasma membranes. *J. Biol. Chem.* 1973; **248**: 5922–5931.
2. Luft FC, Steinberg H, Ganten U, Meyer D, Gless KH, Lang RE, Fineberg NS, Rascher W, Unger T, Ganten D. Effect of sodium chloride and sodium bicarbonate on blood pressure in stroke-prone spontaneously hypertensive rats. *Clin. Sci. (Lond)* 1988; **74**: 577–585.
3. Versteeg CAM, Bohus B, de Jong W. Attenuation by arginine- and desglycinamide-lysine-vasopressin of a centrally evoked pressor response. *J. Autonom. Nerv. Syst.* 1982; **6**: 253–262.
4. Jard S, Gaillard RC, Guillon G, Marie J, Schoenenberg P, Muller AF, Manning M, Sawyer WH. Vasopressin antagonists allow demonstration of a novel type vasopressin receptor in the rat adenohypophysis. *Mol. Pharmacol.* 1986; **30**: 171–177.
5. Wilkinson MF, Kasting NW. The antipyretic effects of centrally administered vasopressin at different ambient temperatures. *Brain Res.* 1987; **415**: 275–280.
6. Wied De D. The influence of the posterior and intermediate lobe of the pituitary and pituitary peptides on the maintenance of a conditioned avoidance response in rats. *Int. J. Neuropharmacol.* 1965; **4**: 157–167.
7. Kendrick KM, Keverne EB, Baldwin BA. Intracerebroventricular oxytocin stimulates maternal behaviour in the sheep. *Neuroendocrinology* 1987; **46**: 56–61.
8. Berkowitz BA, Sherman S. Characterization of vasopressin analgesia. *J. Pharmacol. Exp. Ther.* 1982; **220**: 329–334.
9. Ree Van JM, Wied De D. Effect of neurohypophyseal hormones on morphine dependence. *Psychoneuroendocrinology* 1977; **2**: 35–41.
10. Barberis C, Tribollet E. Vasopressin and oxytocin receptors in the central nervous system. *Crit. Rev. Neurobiol.* 1996; **10**: 119–154.
11. Soloff MS, Pearlmutter AF. Characterization of the metal ion requirement for oxytocin–receptor interaction in rat mammary gland membranes. *J. Biol. Chem.* 1979; **254**: 3899–3906.
12. Schmidt JM, Ohlenschläger O, Rüterjans H, Grzonka Z, Kojro E, Pavo I, Fahrenholz F. Conformation of [Arg^8]vasopressin and V_1 antagonists in dimethylsulfoxide solution derived from two-dimensional NMR spectroscopy and molecular dynamics simulation. *Eur. J. Biochem.* 1991; **201**: 355–371.
13. Hempel JC. The conformation of neurohypophyseal hormones. In *The Peptides: Analysis, Synthesis, Biology*, Smith CW (ed.). Academic Press: New York, 1996; **8**: 209–237.
14. Hruby VJ, Lebl MI. Conformational properties of neurohypophyseal hormone analogs in solution as determined by NMR and laser RAMAN spectroscopies. In *CRC Handbook of Neurohypophyseal Hormone Analogs*, Jost K, Lebl M, Brtnik F (eds). CRC Press: Boca Raton FL, 1997; **1**: 105–155.
15. Krishna NR, Huang DH, Glickson JD, Rowan RI II, Walter R. Amide hydrogen exchange rates of peptides in H2O solution by ^{1}H nuclear magnetic resonance transfer of solvent saturation method. *Biophys. J.* 1979; **26**: 345–366.
16. Fric I. *Handbook of Neurohypophyseal Hormone Analogs*, Jost K, Lebl M, Bratnik F (eds). CRC Press: Boca Raton, 1987; 159.
17. Liwo A, Tempczyk A, Ołdziej S, Shenderovich MD, Hruby VJ, Talluri S, Ciarkowski J, Kasprzykowski F, Łankiewicz L, Grzonka Z. Exploration of the conformational space of oxytocin and arginine-vasopressin using the electrostatically driven Monte Carlo and molecular dynamics methods. *Biopolymers* 1996; **38**: 157–175.
18. Langs DA, Smith GD, Stezowski JJ, Hughes RE. Structure of pressinoic acid: The cyclic moiety of vasopressin. *Science* 1986; **232**: 1240–1242.
19. Mouillac B, Chini B, Balestre M-N, Elands J, Trumpp-Kallmeyer S, Hoflack J, Hibert M, Jard S, Barberis C. The binding site of neuropeptide vasopressin V1a receptor. Evidence for a major localization within transmembrane regions. *J. Biol. Chem.* 1995; **270**: 25771–25777.
20. Czaplewski C, Kaźmierkiewicz R, Ciarkowski J. Vasopressin V2 receptor/bioligand interactions. *Lett. Peptide Sci.* 1998; **5**: 333–335.
21. Czaplewski C, Pasynkiewicz-Gierula M, Ciarkowski J. G Protein-coupled receptor–bioligand interactions modeled in a phospholipid bilayer. *Int. J. Quant. Chem.* 1999; **73**: 61–70.
22. Iwadate M, Nagao E, Williamson MP, Ueki M, Asakura T. Structure determination of [Arg^8]vasopressin methylenedithioether in dimethylsulfoxide using NMR. *Eur. J. Biochem.* 2000; **267**: 4504–4510.
23. Walse B, Kihlberg J, Drakenberg T. Conformation of desmopressin, an analogue of the peptide hormone vasopressin, in aqueous solution as determined by NMR spectroscopy. *Eur. J. Biochem.* 1998; **252**: 428–440.
24. Wang J, Hodges RS, Sykes BD. Effect of trifluoroethanol on the solution structure and flexibility of desmopressin: a two dimensional NMR study. *Int. J. Peptide Protein Res.* 1995; **45**: 471–481.
25. Wang J, Hodges RS, Sykes BD. Errata. *Int. J. Peptide Protein Res.* 1995; **46**: 547.

26. Lippens G, Hallenga K, Van Belle D, Wodak SJ, Nirmala NR, Hill P, Russel KC, Smith DD, Hruby VJ. Transfer nuclear Overhauser effect study of the conformation of oxytocin bound bovine neurophysin I. *Biochemistry* 1993; **32**: 9423–9434.
27. Shenderovich MD, Sekatsis IP, Liepin'sh EE, Nikoforovich G, Papsuevich OS. Study of the spatial structure of des-Gly^9-[Arg^8]vasopressin by two-dimensional NMR spectroscopy and theoretical conformation analysis. *Bioorg. Khim.* 1985; **11**: 1180–1191.
28. Yu C, Yang TH, Yeh CJ, Chuang LC. Combined use of NMR, distance geometry, and restrained energy minimization for the conformational analysis of 8-lysine-vasopressin. *Can. J. Chem.* 1992; **70**: 1950–1955.
29. Shenderovich MD, Kasprzykowski K, Liwo A, Sekacis IP, Saulitis J, Nikiforovich GV. Conformational analysis of [Cpp^1, Sar^7, Arg^8] vasopressin by 1H-NMR spectroscopy and molecular mechanics calculations. *Int. J. Peptide Protein Res.* 1991; **38**: 528–538.
30. Zieger G, Andreae F, Sterk H. Assigment of proton NMR resonances and conformational analysis of [Lys^8]-vasopressin homologues. *Magn. Reson. Chem.* 1991; **29**: 580–586.
31. Nutz KI, Fabian WM, Sterk H. Conformations of triglycyl-lysylvasopressin: ^{1}H NMR spectroscopic and molecular dynamics study. *Magn. Reson. Chem.* 1993; **31**: 481–488.
32. Grzonka Z, Mishra PK, Bothner-by AA. Conformational preferences and binding to neurophysins of oxytocin analogs with sarcosine or *N*-methylalanine in position 7. *Int. J. Peptide Protein Res.* 1985; **25**: 375–381.
33. Botos CR, Smith CW, Chan VL, Walter R. Synthesis and biological activities of arginine-vasopressin analogues designed from a conformation-activity approach. *J. Med. Chem.* 1979; **22**: 926–931.
34. Kolc J, Zaoral M, Šorm F. Amino acids and peptides. LXXV. Synthesis of [Gly^7,Lys^8]vasopressin and [D-Pro^7,Lys^8]vasopressin. *Coll. Czech. Chem. Commun.* 1967; **32**: 2667–2671.
35. Cort J, Schück OS, Stribrna J, Skopova J, Jast K, Mulder IL. Role of the disulfide bridge and the C-terminal tripeptide in the antidiuretic action of vasopressin in man and the rat. *Kidney Int.* 1975; **8**: 292–302.
36. Kasprzykowski F, Grzonka Z, Melin P. [Gly^7]AVP and [1-β-mercaptopropionic acid]AVP, [Gly^7]AVP, two analogs with high hormonal selectivity. *Polish J. Chem.* 1987; **61**: 641–644.
37. Li CH. Studies on pituitary lactogenic hormone. XVII. Oxidation of the ovine hormone with performic acid. *J. Biol. Chem.* 1957; **229**: 157–163.
38. Grzonka Z, Lammek B, Kasprzykowski F, Gazis D, Schwartz IL. Synthesis and some pharmacological properties of oxytocin and vasopressin analogues with sarcosine or *N*-methyl-L-alanine in position 7. *J. Med. Chem.* 1983; **26**: 555–559.
39. Liwo A, Tempczyk A, Ołdziej S, Shenderovich MD, Hruby VJ, Talluri S, Ciarkowski J, Kasprzykowski F, Łankiewicz L, Grzonka Z. Exploration of the conformational space of oxytocin and arginine-vasopressin using the electrostatically driven Monte-Carlo and molecular dynamics methods. *Biopolymers* 1996; **38**: 157–175.
40. Groth M, Malicka J, Czaplewski C, Liwo A, Łankiewicz L, Wiczk W. Maximum entropy approach to the determination of solution conformation of flexible polypeptides by global conformational analysis and NMR spectroscopy — application to DNS^1-c[D-A$_2$bu^2, Trp^4, Leu^5]-enkephalin and DNS^1-c[D-A$_2$bu^2, Trp^4, D-Leu^5]-enkephalin. *J. Biomol. NMR* 1999; **15**: 315–330.
41. Grzonka Z, Kasprzykowski F, Kojro E, Darłak K, Melin P, Fahrenholz F, Crause P, Boer R. Arginine-vasopressin analogues with high antidiuretic/vasopressor selectivity. Synthesis, biological activity and receptor affinity of arginine-vasopressin analogues with substitutions in positions 1, 2, 4, 7 and 8. *J. Med. Chem.* 1986; **29**: 96–99.
42. Bax A, Freeman R. Enhanced NMR resolution by restricting the effective sample volume. *J. Magn. Reson.* 1985; **65**: 355–360.
43. Bothner-By AA, Stephens RL, Lee J-M, Warren CD, Jeanloz RW. Structure determination of a tetrasaccharide: Transient nuclear Overhauser effects in the rotating frame. *J. Am. Chem. Soc.* 1984; **106**: 811–813.
44. Bax A, Davis DG. Practical aspects of two-dimensional transverse NOE spectroscopy. *J. Magn. Reson.* 1985; **63**: 207–213.
45. Kay LE, Keifer P, Saarinen T. Pure absorption gradient enhanced heteronuclear single quantum correlation spectroscopy with improved sensitivity. *J. Am. Chem. Soc.* 1992; **114**: 10663–10665.
46. Palmer III AG, Cavanagh J, Wright PE, Rance M. Sensitivity improvement in proton-detected two-dimensional heteronuclear correlation NMR spectroscopy. *J. Magn. Reson.* 1991; **93**: 151–170.
47. Kontaxis G, Stonehouse J, Laue ED, Keeler J. The sensitivity of experiments which use gradient pulses for coherence-pathway selection. *J. Magn. Reson. Ser. A* 1994; **111**: 70–76.
48. Hoffman RE, Davies DB. Temperature dependence of NMR secondary references for D_2O and $(CD_3)_2SO$ solutions. *Magn. Reson. Chem.* 1998; **26**: 523–525.
49. Bartles C, Xia T, Billeter M, Günter P, Wütrich K. The program XEASY for the computer-supported NMR spectral analysis of biological macromolecules. *J. Biomol. NMR* 1995; **5**: 1–10.
50. Koźmiński W. A pure-phase homonuclear J-modulated HMQC experiment with tilted cross-peak patterns for an accuracy determination of homonuclear couplings. *J. Magn. Reson.* 1999; **141**: 185–190.
51. Koźminski W. The new active-coupling-pattern tilting experiment for an efficient and accurate determination of homonuclear coupling constants. *J. Magn. Reson.* 1998; **134**: 189–193.

52. Güntert P, Braun W, Billeter M, Wüthrich K. Automated stereospecific ^{1}H NMR assignments and their impact on the precision of protein structure determination in solution. *J. Am. Chem. Soc.* 1989; **111**: 3997–4004.
53. Güntert P, Wüthrich K. Improved efficiency of protein structure calculation NMR data using program DIANA with redundant dihedral angle constraints. *J. Biomol. NMR* 1991; **1**: 447–456.
54. Bystrov VF. Spin-spin coupling and the conformational states of peptide systems. *Progr. NMR Spectrosc.* 1976; **10**: 41–81.
55. Güntert P, Wüthrich K. Efficient computation of three-dimensional protein structures in solution from nuclear magnetic resonance data using the program DIANA and the supporting programs CALIBA, HABAS and GLOMSA. *J. Mol. Biol.* 1991; **217**: 517–530.
56. Ripoll DR, Scheraga HA. On the multiple-minima problem in the conformational analysis of polypeptides. II. An electronically driven Monte carlo method — tests on poly(L-alanine). *Biopolymers* 1988; **27**: 1283–1303.
57. Némethy G, Gibson KD, Palmer KA, Yoon CN, Paterlini G, Zagari A, Rumsey S, Scheraga HA. Energy parameters in polypeptides. 10. Improved geometrical parameters and nonbonded interactions for use in the ECEPP/3 algorithm with application to proline-containing peptides. *J. Phys. Chem.* 1992; **96**: 6472–6484.
58. Brünger AT. *The X-PLOR Software Manual. Version 3.1.* Yale University Press: New Haven, CT, 1992.
59. Vila J, Williams RL, Vásquez M, Scheraga HA. Empirical solvation models can be used to differentiate native from near-native conformations of bovine pancreatic trypsin inhibitor. *Proteins Struct. Funct. Genet.* 1991; **10**: 199–218.
60. Ripoll DR, Pottle MS, Gibson KD, Liwo A, Scheraga HA. Implementation of the ECEPP algorithm, the Monte Carlo minimization method. *J. Comput. Chem.* 1995; **16**: 1153–1163.
61. Späth H. Cluster analysis algorithms. *J. Comput Chem.* 1980; **10**: 209–220.
62. Massefski W Jr, Bolton PH. Quantitative analysis of nuclear Overhauser effects. *J. Magn. Reson.* 1985; **65**: 526–530.
63. Meadows RP, Post CB, Luxon BA, Gorenstein DG. *MORASS 2.1.* Purdue University: West Lafayette, 1994.
64. Post CB, Meadows RP, Gorenstein DG. On the evaluation of interproton distance for 3-dimensional structure determination by NMR using a relaxation rate matrix analysis. *J. Am. Chem. Soc.* 1990; **112**: 6796–6803.
65. Bhaskaran R, Chuang L-C, Yu C. Conformational properties of oxytocin in dimethyl sulfoxide solution: NMR and restrained molecular dynamics studies. *Biopolymers* 1992; **32**: 1599–1608.
66. Brooks B, Bruccoleri R, Olafson BO, States DJ, Swaminathan S, Karplus M. CHARMM: a program for macromolecular energy, minimization and dynamics calculations. *J. Comp. Chem.* 1993; **4**: 187–217.
67. Powell MJD. Restart procedures for conjugate gradient method program. *Math. Prog.* 1977; **12**: 241–254.
68. Koradi R, Billeter M, Wüthrich K. MOLMOL: a program for display and analysis of macromolecular structures. *J. Mol. Graphics* 1996; **14**: 52–55.
69. Lewis PN, Mamony FA, Sheraga HA. Chain reversals in proteins. *Biochem. Biophys. Acta* 1973; **303**: 211–229.
70. Liwo A, Tempczyk A, Grzonka Z. Molecular mechanics calculations on deaminooxytocin and on deaminoarginine-vasopressin and its analogues. *J. Comput. Aided Mol. Design* 1989; **2**: 281–309.
71. Schertler GFX, Villa C, Henderson R. Projection structure of rhodopsin. *Nature* 1993; **362**: 770–772.

